Clinical Biomechanics 29 (2014) 1–6

Contents lists available at ScienceDirect

Clinical Biomechanics

journal homepage: www.elsevier.com/locate/clinbiomech

The Clinical Biomechanics Award 2013 – presented by the International Society of Biomechanics: New observations on the morphology of the talar dome and its relationship to ankle kinematics

Sorin Siegler [a,*], Jason Toy [b], Damani Seale [b], David Pedowitz [c]

[a] Department of Mechanical Engineering and Mechanics, Drexel University, 32nd and Chestnut Streets, Philadelphia, PA 19104, USA
[b] Department of Mechanical Engineering and Mechanics, Drexel University, Philadelphia, PA, USA
[c] The Rothman Institute, Thomas Jefferson University, Philadelphia, PA, USA

ARTICLE INFO

Article history:
Received 19 June 2013
Accepted 15 October 2013

Keywords:
Talus
Trochlear surface
Functional morphology
Truncated cone
Saddle shape
Ankle kinematics

ABSTRACT

Background: Ankle passive kinematics is determined primarily by articular surface morphology and ligament constraints. Previous morphological studies concluded that the talar dome can be approximated by a truncated cone, whose apex is directed medially and whose major axis is the axis of rotation of the ankle. This and other functional morphology concepts were evaluated in this study whose goal was to describe and quantify the 3D morphology of the talus using 3D image-based bone models and engineering software tools.
Methods: CT data from 26 healthy adults were processed to produce 3D renderings of the talus and were followed by morphological measurements including the radii of curvature of circles fitted to the medial and lateral borders of the trochlea and radii of curvature of coronal sections.
Findings: The surfaces containing the medial and lateral borders of the trochlea are not parallel and the radius of curvature of the medial border is larger than the lateral border. In the coronal plane the trochlear surface was mostly concave.
Interpretation: The trochlear surface can be modeled as a skewed truncated conic saddle shape with its apex oriented laterally rather than medially as postulated by Inman. Such shape is compatible, as opposed to Inman's cone postulate, with the observed pronation/supination and provides stable congruency in movements of inversion/eversion. The results challenge the fundamental theories of functional morphology of the ankle and suggest that these new findings should be considered in future biomechanical research and in clinical applications such as design of total ankle replacements.

1. Introduction

The passive kinematic properties of the ankle are the result of a complex interaction between bony articular morphology and ligament constraints. The basic patterns of motion however, are primarily determined by the geometric features of the articulating surfaces of the talus, and of the tibia and fibula, i.e. the trochlear surface and the tibial/fibular mortise.

Some of the first detailed studies of the functional morphology of the trochlea were conducted more than 60 years ago (Barnett and Napier, 1952; Close, 1956; Close and Inman, 1952; Hicks, 1953; Sewell, 1904) and included the seminal work by Inman and Close and their co-workers. At that time, most investigators regarded the talocrural joint as a one-degree of freedom joint with a fixed axis of rotation. Relying on the fixed axis of rotation assumption, Inman and his co-workers (Close, 1956; Close and Inman, 1952; Inman, 1976) then performed detailed morphological measurements on cadaver specimens and concluded that the trochlear surface of the talus can be represented as a frustum of a cone, whose apex is directed medially and whose major axis coincides (or actually forced to coincide) with the line connecting the tips of the medial and lateral malleolus (Close and Inman, 1952; Inman, 1976). Since Inman's original studies, despite the fact that the concept of a fixed axis of rotation for the ankle has been refuted by many studies (Barnett and Napier, 1952; Hicks, 1953; Lundberg et al., 1989; Sammarco, 1977; Siegler et al., 1988) and despite the apparent contradiction with experimental observations on ankle coupled behavior of pronation/supination (Close and Inman, 1952; de Asla et al., 2006; Siegler et al., 1988), the idea of a truncated cone with its apex directed medially, is still, to a large extent, accepted by experts in this field (Hintermann et al., 2004; Stiehl, 1991). In fact, this idea has been implemented in recent years in the geometry of surfaces of some modern total ankle replacements (Bonnin et al., 2004; Hintermann et al., 2004), clearly demonstrating the importance of this concept to the clinical management of ankle disorders. However, the validity of this concept becomes doubtful in light of the fact that it relies entirely on an assumed fixed axis of rotation for the ankle, shown, as indicated

* Corresponding author.
E-mail address: ssielger@coe.drexel.edu (S. Siegler).

0268-0033/$ – see front matter © 2013 Elsevier Ltd. All rights reserved.
http://dx.doi.org/10.1016/j.clinbiomech.2013.10.009

earlier, to be invalid. Therefore, the main goal of the present study was to provide a detailed description of the 3D morphology of the talus using 3D image-based bone models and engineering software tools unconstrained by the assumption of a fixed axis of rotation for the ankle. The results were then be used to evaluate Inman's truncated cone concept and other functional morphological concepts such as the curvature of the trochlea in the frontal plane.

2. Methods

The study was performed on CT data from 26 healthy ankles obtained from 26 individuals ranging in age between 18 and 35 years. The CT data was collected with a resolution of $0.5 \times 0.5 \times 1.5$ mm. All identifying data such as patient name and name of referring physician were removed from the DICOM files prior to being made available to the study from the Rothman Institute, Philadelphia, PA. The CT data from each ankle was imported into commercial image processing software (Analyze Direct™) to produce three dimensional numerical renderings of the bones articulating at the ankle joint consisting of the talus, the distal tibia and the distal fibula. The bone renderings were obtained by the process of segmentation, an edge detection algorithm for identifying the boundaries of each bone in each 2D slice, followed by 3D rendering algorithm in which the 2D segmented images were combined to produce surface representation of the talus, the distal tibia and the distal fibula. The 3D surface renderings were then exported from Analyze Direct™ for use in commercial, 3D CAD and reverse engineering software — Geomagic™ where they were slightly smoothed through a spatial filter to remove minor spikes introduced during the segmentation process (Fig. 1). All subsequent 2D and 3D processing and measurements were performed in both Geomagic™ and in AUTODESK INVENTOR™.

The general dimensions of length, height and width of each talus were recorded from the CAD environment as the dimensions of a "bounding box" which defined the extents of the talus across its major axes (Fig. 2).

Three near sagittal sections were created through the talus. A medial section was first selected manually so as to contain the medial shoulder of the trochlear surface of the talus representing the border between the medial side of the trochlear surface and the medial facet (MFP line in Fig. 1). A lateral section was then created by shifting a plane laterally, parallel to the medial section and then rotating this plane about a superior-to-inferior line so as to contain the lateral shoulder of the trochlear surface representing the border between the lateral side of the trochlea and the lateral facet (LFP line in Fig. 1). The angle between these two planes was measured. The width of the trochlea, W was defined and measured between the medial and lateral sections at the central coronal section (Fig. 1). The third sagittal section, the central section, was created by shifting a plane parallel to the medial section through a distance equal to half of the width W of the trochlea and

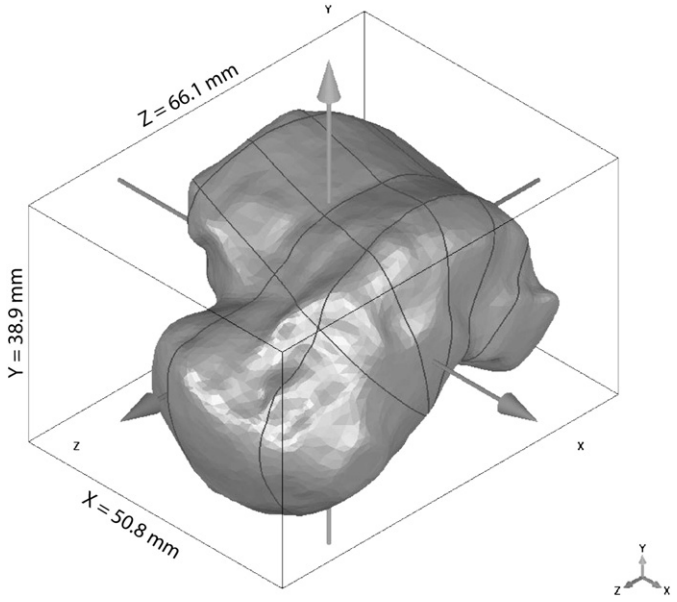

Fig. 2. An example of the general dimensions of the talus of width (X-dimension), height (Y-dimension) and length (Z-dimension) recorded as the boundary dimensions of a "bounding box".

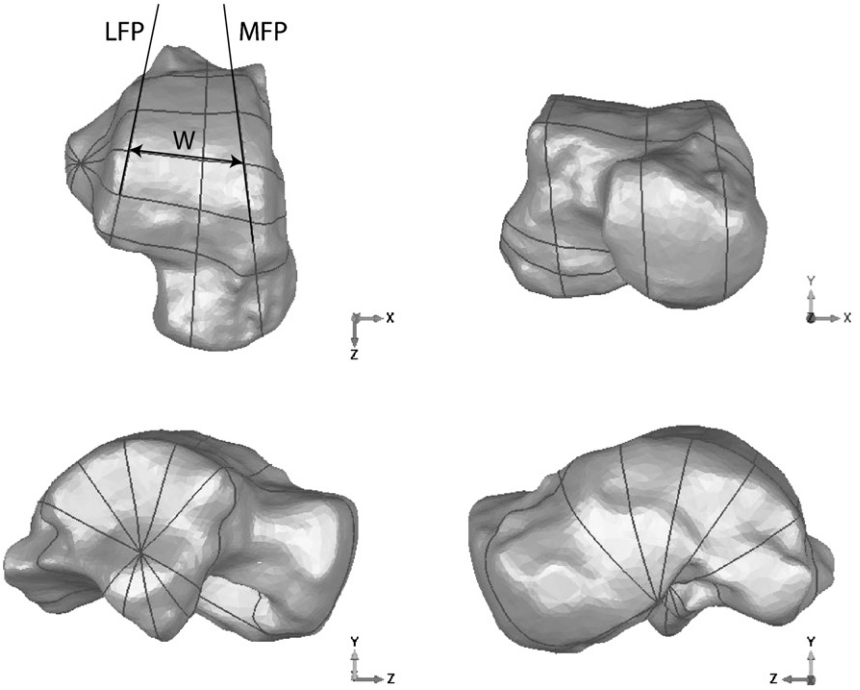

Fig. 1. Views (clockwise from top left: superior, frontal, medial and lateral) of the talus in the CAD environment (Geomagic™). Line LFP (lateral facet plane) and line MFP (medial facet plane) represent the medial and lateral facet sections through the trochlea. W represents the width of the trochlea measured at the central coronal section.

then rotating this plane about a superior/inferior axis so as to bisect the angle between the medial and lateral sections (Fig. 3). In each of these sections, optimal circles, in the least-square error sense, were fitted to the contour of the trochlea between the anterior and posterior boundaries (Fig. 3). In addition, the angle formed between the line perpendicular to the medial section passing through the center of the circle, line B–B (Fig. 4) and the line connecting the centers of the medial and lateral circles, line A–A (Fig. 4) was recorded for each talus. The angles between these two lines when projected onto a coronal plane and onto a transverse plane were also computed. In each 3D rendering, the line connecting the tips of the medial and lateral malleolus was identified, line C–C (Fig. 4) and the angle formed between this line and the line connecting the medial and lateral best-fitted circles, line A–A was measured (Fig. 4).

Five equally spaced sections, between the anterior and posterior trochlear boundaries, were produced through the talus by rotating coronal planes about the line connecting the centers of the medial and lateral circles which were fitted earlier to the medial and lateral trochlear boundaries (Fig. 5). Optimal (in the least-square error sense) circles were then fitted to the contour of the trochlea between the medial and lateral boundaries in each of these five sections (Fig. 5).

An ANOVA statistical analysis followed (if the ANOVA indicates significant differences at $P < 0.05$) by a Newman–Keuls post-hoc test was performed to explore differences between the three radii of the best-fitted circles in the sagittal plane and the five best-fitted radii in the coronal plane of the talus.

3. Results

The general dimensions of the talus as measured by the size of the bounding box (Fig. 2) were: length — average 65.15 mm, standard deviation 6.6 mm; width — average 48.4 mm, standard deviation 7.2 mm; and height — average 41.7 mm, standard deviation of 5.7 mm. The trochlea had an average width of W = 24.8 mm with a standard deviation of 2.8 mm measured at the central coronal section (Fig. 1). The angle formed between the medial and lateral facets (Fig. 1) measured an average of 9.9° with a standard deviation of 4.1°. The apex of this angle was oriented posteriorly, indicating that the trochlea is wider on its anterior part than on its posterior part.

The radius of curvature of the circle fitted to the medial facet of the talus in the sagittal plane had an average value of 25.7 mm and a standard deviation of 4.8 mm. It was larger, but without statistically significance ($P > 0.05$), than the radius of the central circle by 1 mm (average = 24.7 mm, standard deviation = 3.8 mm) and was significantly larger ($P = 6.5 \times 10^{-5}$) by an average of 4 mm than the radius of curvature of the circle fitted to the lateral facet, which had an average radius of 21.7 mm with a standard deviation of 2.9 mm (Fig. 3). The angle by which the line connecting the centers of the medial and lateral circles, line A–A (Fig. 4) was offset from a line perpendicular to the medial circle at its center, line B–B (Fig. 4) had an average value of 20.9° and a standard deviation of 16.7°. The angle between these two lines when projected onto the coronal plane had an average value of 18.7° with a standard deviation of 17.6° and when projected onto a transverse plane had an average value of 9.4° with a standard deviation of 10.2°. Finally, the angle between the line connecting the centers of the best-fitted medial and lateral circles, line A–A (Fig. 4) and the line connecting the tips of the medial and lateral malleolus, line C–C (Fig. 4) had an average value of 16° with a standard deviation of 6.3°.

In the coronal plane, the radius of curvature of circles fitted to the trochlear contours (Fig. 5), increases from anterior, where it is the smallest to posterior, where it is almost flat (average and standard deviation values (shown in parentheses) were: anterior, 31.6 (23) mm; antero-central, 63.6 (26) mm, central, 70.2 (26) mm; postero-central, 87 (39) mm; and posterior, 111.9 (43 mm)). However, large variations in this trend were observed towards the posterior side of the trochlea where some coronal contours were slightly concave, some virtually flat and some slightly convex.

4. Discussion

A three dimensional functional morphology study of the talus was conducted using 3D image processing and engineering software tools in order to revisit Inman's concept, made more than 60 years ago

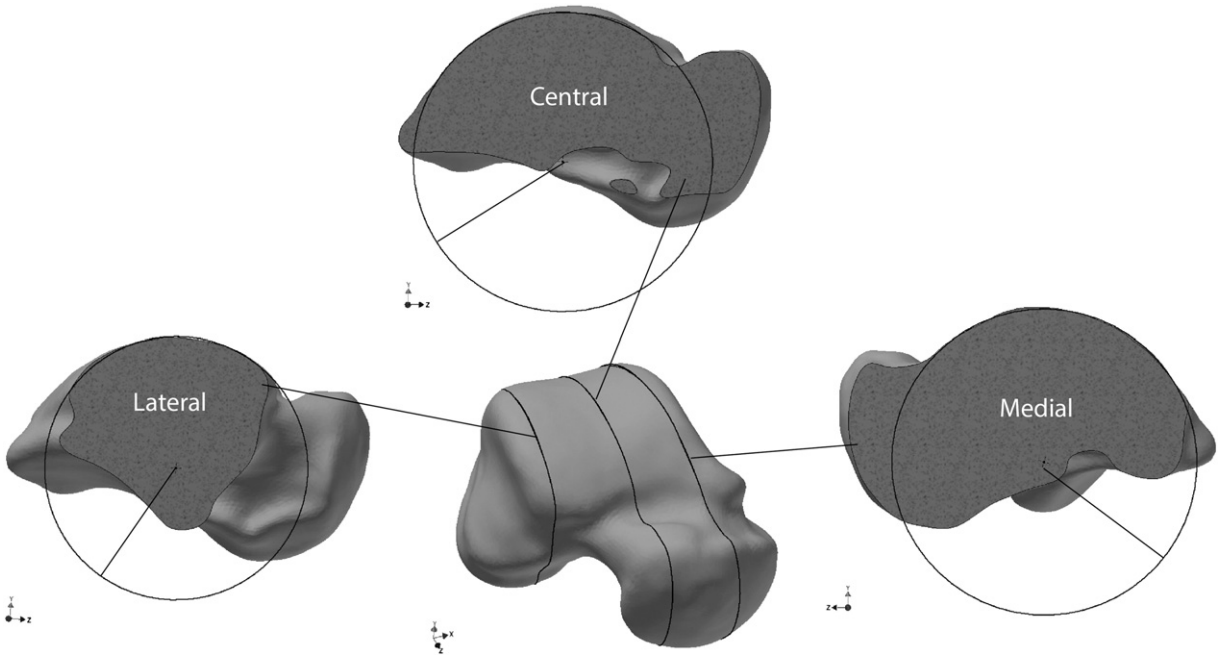

Fig. 3. Sagittal sections through the talus coinciding with: the medial facet; the lateral facet; and a central section created by shifting a plane parallel to the medial section through a distance equal to half of the width of the trochlea and rotating it about a superior/inferior axis so as to bisect the angle between the medial and lateral sections. Each sagittal section shows the best-fitted circle to the trochlear contour between its anterior and posterior boundaries.

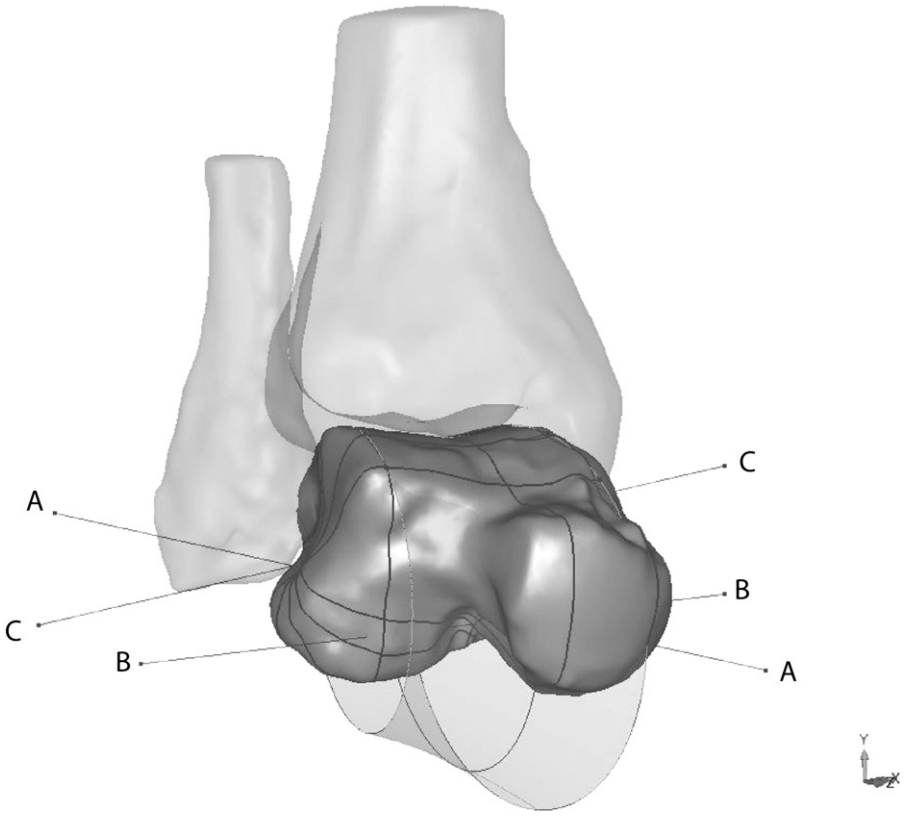

Fig. 4. An isometric view of the ankle showing the trochlear surface to be part of the surface of a skewed truncated cone with its apex oriented laterally and a concave surface in the coronal plane resulting in a truncated conic saddle shape. Line A–A connects the centers of the best-fitted medial and lateral circles, considered the axis of the cone. Line B–B is the perpendicular to the surface of the medial circle at its center. Line C–C is the line connecting the tips of the medial and lateral malleoli.

(Close and Inman, 1952; Inman, 1976), that the trochlear surface of the talus can be approximated by a truncated cone with its apex located medially. This concept was established based on curvature measurements of the medial and lateral facets of the trochlea of talus obtained from cadaver specimens using three different precision manual measuring devices. On the basis of these measurements Inman and co-workers observed, after fitting circular arcs to the medial and lateral facets of the talus, that the medial facet had a smaller radius of curvature than the lateral facet (Inman, 1976). Earlier (Close and Inman, 1952), a specially designed holder and saw guide tool that produced cuts into the

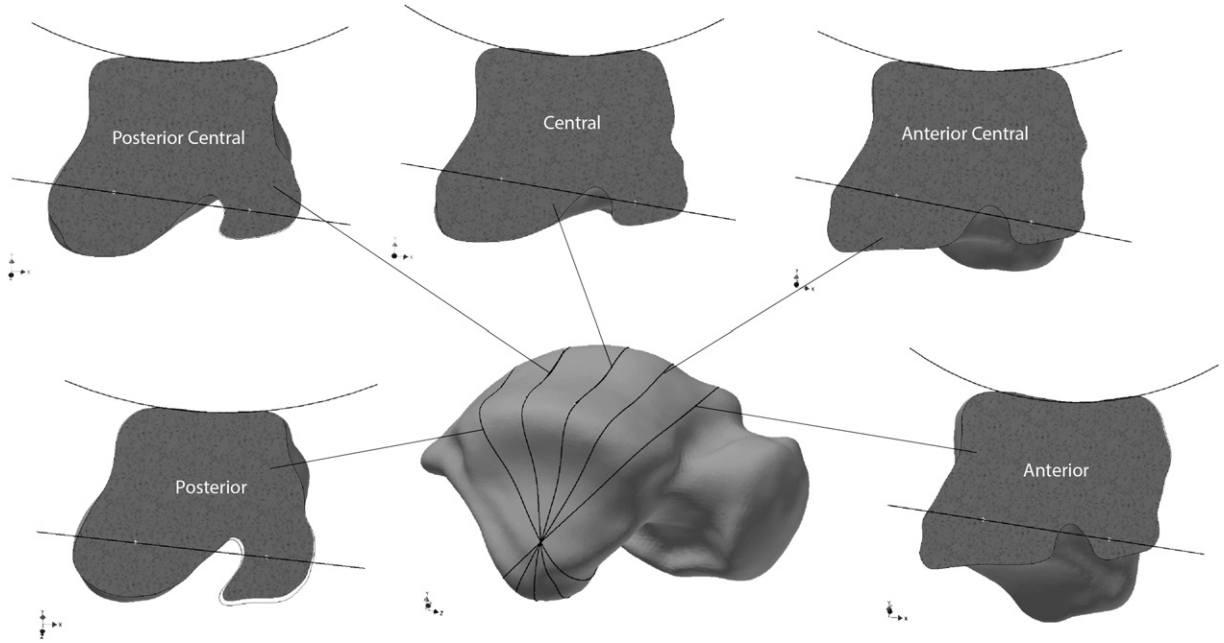

Fig. 5. Five equally spaced sections produced through the talus by rotating coronal planes about a line connecting the centers of the medial and lateral circles (line A–A). These planes are rotated between the anterior and posterior borders of the trochlea. Each coronal section shows the best-fitted circle to the trochlear contour between its medial and lateral borders.

trochlear surface were used to evaluate qualitatively the geometrical characteristics of the trochlear surface. In that study it was observed that the saw cut lines, produced on the surface of the trochlea, converged on the medial side of the talus (Close and Inman, 1952) suggesting a truncated cone with a medially oriented apex. Although different in their specific features, all these techniques relied on one common assumption of a fixed axis of rotation for the ankle approximated by a line connecting the tips of the lateral and medial malleolus. On the basis of his truncated cone concept Inman explained (Close and Inman, 1952) that such a shape (conic surface with apex directed medially) has to produce external rotation as the ankle moves from dorsiflexion into plantarflexion and vice versa, internal rotation as the ankle moves into dorsiflexion. However, this assumed coupled behavior was inconsistent with his observations made in the same study of normal subjects during level walking. There he noticed that internal rotation was coupled with plantarflexion and external rotation with dorsiflexion. This observed coupled behavior was fully consistent with the well-known pronation/supination motion which was observed and quantified by him (Close and Inman, 1952) and by others (de Asla et al., 2006; Siegler et al., 1988). Inman attempted to resolve the apparent conflict between experimental observations and his cone postulate not by casting a doubt on the later but by suggesting that the horizontal torque acting on the foot during gait was strong enough to reverse the natural coupled behavior of the ankle (Close and Inman, 1952).

The functional morphology concept produced based on the results obtained in the present study is directly opposite to the Inman's concept of a truncated cone with its apex located medially. According to the present results the trochlear surface of the talus can be modeled as a truncated cone with its apex directed laterally since the radius of curvature of the circle fitted to the lateral border of the talar dome is significantly smaller than that of the medial border. This truncated cone is skewed since the line joining the medial and lateral fitted circles is not perpendicular to the medial fitted circle, which serves as the base of the cone (Fig. 4). The reason for the contradiction between the functional morphology concepts of the present study and that of Inman is in the reliance on an assumed fixed axis of rotation. Inman and his co-workers fully relied on an assumed one degree of freedom fixed axis of rotation passing just below the tips of the medial and lateral malleolus. As described earlier, this assumption was shown to be incorrect by several investigators (Barnett and Napier, 1952; Hicks, 1953; Leardini et al., 1999; Lundberg et al., 1989; Sammarco, 1977; Siegler et al., 1988) who found that no such fixed axis of rotation exists. No such assumption was applied in the present study which relied solely on the 3D geometrical features of the talar dome obtained through CT imaging, imaging techniques which were unavailable to Inman and his co-workers in the fifties.

An important functional implication of this study's findings is that a truncated cone with its apex located laterally is consistent with the well-known kinematic coupling behavior of the ankle joint known as pronation/supination, i.e., as the ankle moves into plantarflexion it moves into internal rotation and inversion (Close and Inman, 1952; de Asla et al., 2006; Siegler et al., 1988; Wong et al., 2005). Another finding of the present study with significant functional implication is that the cone representing the trochlear surface is skewed and therefore lacks an axis of symmetry. Such lack of an axis of symmetry implies a continuously varying axis of rotation, a conclusion which is in full accord with most previous experimental observations (Lundberg et al., 1989; Sammarco, 1977; Siegler et al., 1988; Stiehl, 1991). The results suggest that this cone is skewed superiorly and slightly posteriorly (Fig. 4) although the values of these offsets varied between subjects. It was further demonstrated that the central line of the skewed cone (the line connecting the centers of the best-fitted medial and lateral circles) does not coincide with the inter-malleolar line, assumed by Inman to be the fixed axis of rotation of the ankle. Finally, it was found that in the coronal plane the trochlear surface is concaved with a diminishing degree of concavity from anterior to posterior direction. This suggests that some amount of independent inversion/eversion motion can occur at the ankle joint on a stable and congruent saddle-like surface and this can occur primarily when the ankle is in dorsiflexion or neutral since the saddle-like surface becomes flat towards plantarflexion. This further implies that the ankle joint not only has a variable axis of rotation but also possesses at least two rotational degrees of freedom as is the case with any saddle-shaped surface. This assertion has been confirmed experimentally by previous investigators (de Asla et al., 2006; Siegler et al., 1988; Wong et al., 2005) and it stands in contrast with previous studies (Leardini et al., 1999) that assumed the ankle to act as a one degree of freedom system with a varying axis of rotation.

This study has some limitations. One limitation is related to the inaccuracies in the morphological measurements that may result from the manual and somewhat subjective selection of both the near sagittal sections as well as from defining the anterior and posterior borders of the trochlear surface for the purpose of spacing the coronal sections. This subjectivity is virtually unavoidable considering the inherent irregularity and variability of anatomical surfaces. However, the relatively slow changing curvature of the trochlear surface and the careful definition of the selection of the various sections used in the present analysis suggest minimum influence of user bias or level of experience on the measured morphological parameters and thus not affecting the study's main conclusions. The second limitation of the study was related to the reliance on CT data to develop the 3D numerical models. These models produced bone surface morphology of the trochlea and did not capture articular surface morphology which would have required visualization and segmentation of the articular cartilage layer. The thickness of the articular cartilage layer of the trochlea was shown in the past to be small, averaging 1.35 mm in males and 1.11 in females (Sugimoto et al., 2005). More importantly and relevant to the present morphological study, the articular cartilage thickness varies only slightly, by less than 0.2 mm, between the medial, lateral and central regions of the talar dome (Sugimoto et al., 2005). Therefore it is anticipated that failing to include the articular cartilage layer would produce only small errors in the calculated morphological parameters without affecting the conclusions of the study.

Detailed knowledge of the morphological characteristics of the articulating surfaces of the ankle joint and their relationship to ankle kinematics is critical for clinical applications such as ankle reconstruction following intra-articular fractures requiring osteochondral grafting of large areas of the talus (i.e., osteochondral defects or avascular necrosis) and design of implant components for total ankle replacements (Hintermann et al., 2004; Kempson et al., 1975; Leardini et al., 2004). Inman's postulate that the trochlear surface can be modeled as a truncated cone with its apex oriented medially has been implemented in some of these clinical applications such as in the design and construction of articular surfaces for some total ankle replacement systems. The results of the present study represent a paradigm shift in understanding the functional morphology of the talus and implementation of these new functional morphological concepts in clinical application such as design of total ankle replacements may produce closer to normal biomechanical joint functionality thus possibly resulting in higher long-term success rates for this clinical procedure. A future study is planned to investigate, both through numerically models of the ankle (Imhauser et al., 2008) and experimentally on cadavers the effect of changes in the morphology of the talus on the three dimensional kinematic characteristics of the ankle.

5. Conclusions

From the results of this image-based morphological study it was concluded that the trochlear surface of the talus can be modeled as a skewed truncated conic saddle shape with its apex oriented laterally. This conclusion is compatible with the observed pronation/supination

motion of the ankle and provides a stable congruency in movements of inversion/eversion. The results of this investigation and the conclusion based on them challenge the fundamental theory of functional morphology of the ankle pioneered by Inman of a truncated cone with apex oriented medially and suggest that these new findings should be considered in future biomechanical research and in clinical applications such as the design of total ankle replacement components and in the surgical reconstruction of talar articular geometry.

Acknowledgment

The contribution of the CT scans by the Rothman Institute, Philadelphia, PA is gratefully acknowledged.

References

Barnett, C.H., Napier, J.R., 1952. The axis of rotation at the ankle joint in man, its influence upon the form of the talus and mobility of the fibula. J. Anat. 86, 1–9.
Bonnin, M., Judet, T., Colombier, J.A., Buscayret, F., Graveleau, N., Piriou, P., 2004. Midterm results of the Salto total ankle prosthesis. Clin. Orthop. Relat. Res. 6–18.
Close, J.R., 1956. Some applications of the functional anatomy of the ankle joint. J. Bone Joint Surg. 38-A, 761–781.
Close, J.R., Inman, V.T., 1952. The action of the ankle joint Prosthetic Devices Research Project. Institute of Engineering Research, University of California, Berkeley.
De Asla, R.J., Wan, L., Rubash, H.E., Li, G., 2006. Six DOF in vivo kinematics of the ankle joint complex: application of a combined dual-orthogonal fluoroscopic and magnetic resonance imaging technique. J. Orthop. Res. 24, 1019–1027.
Hicks, J.H., 1953. The mechanics of the foot I, the joints. J. Anat. 87, 345–357.
Hintermann, B., Valderrabano, V., Dereymaeker, G., Dick, W., 2004. The HINTEGRA ankle: rationale and short-term results of 122 consecutive ankles. Clin. Orthop. Relat. Res. 57–68.
Imhauser, C.W., Siegler, S., Udupa, J.K., Toy, J.R., 2008. Subject-specific models of the hindfoot reveal a relationship between morphology and passive mechanical properties. J. Biomech. 41, 1341–1349.
Inman, V.T., 1976. The Joints of the Ankle. Williams&Wilkins, Baltimore.
Kempson, G.E., Freeman, M.A., Tuke, M.A., 1975. Engineering considerations in the design of an ankle joint. Biomed. Eng. 10 (166–71), 80.
Leardini, A., O'Connor, J.J., Catani, F., Giannini, S., 1999. A geometric model of the human ankle joint. J. Biomech. 32, 585–591.
Leardini, A., O'Connor, J.J., Catani, F., Giannini, S., 2004. Mobility of the human ankle and the design of total ankle replacement. Clin. Orthop. Relat. Res. 39–46.
Lundberg, A., Svensson, O.K., Nemeth, G., Selvik, G., 1989. The axis of rotation of the ankle joint. J Bone Joint Surg Br 71, 94–99.
Sammarco, J., 1977. Biomechanics of the ankle. I. Surface velocity and instant center of rotation in the sagittal plane. Am. J. Sports Med. 5, 231–234.
Sewell, R.B.S., 1904. A study of the astragalus. J. Anat. Physiol. 38.
Siegler, S., Chen, J., Schneck, C.D., 1988. The three-dimensional kinematics and flexibility characteristics of the human ankle and subtalar joints — part I: kinematics. J. Biomech. Eng. 110, 364–373.
Stiehl, J.B., 1991. Inman's Joints of the Ankle. Williams& Wilkins, Baltimore.
Sugimoto, K., Takakura, Y., Tohno, Y., Kumai, T., Kawate, K., Kadono, K., 2005. Cartilage thickness of the talar dome. Arthroscopy 21, 401–404.
Wong, Y., Kim, W., Ying, N., 2005. Passive motion characteristics of the talocrural and the subtalar joint by dual Euler angles. J. Biomech. 38, 2480–2485.